

ELECTROCHEMICAL SYNTHESIS OF CuTCNQF AND EVALUATION OF ITS CATALYTIC ACTIVITIES

Received:

15 – 09 – 2018

Accepted:

25 – 11 – 2018

<http://jshe.ued.udn.vn/>

Vo Thang Nguyen^{a*}, Tran Duc Manh^a, Dinh Thi Sen^b

Abstract: Cyclic voltammetry experiments were conducted to investigate the first TCNQF^{0/-} reduction processes occurring in solutions containing TCNQF and [Cu(MeCN)₄]⁺. The experiments showed that this process could be monitored without any interference from the second one. During this process, the formation of the solid CuTCNQF was recorded at a concentration of 8.0 mM for TCNQF and [Cu(MeCN)₄]⁺. Noticeably, during the experiments, the generation of two different morphologies of CuTCNQF was observed via an additional irreversible CV wave. This material was successfully synthesized chemically and electrochemically and was characterized using the IR and Raman spectroscopy. CuTCNQF, unlike other fluoro derivatives, did not possess good catalytic activity on Fe³⁺/S₂O₈²⁻ redox reaction. The reaction rate with the presence of CuTCNQF was as slow as it was in the presence of CuTCNQ phase II.

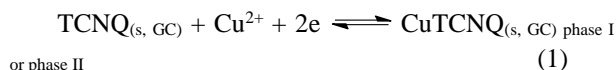
Key words: TCNQF; [Cu(MeCN)₄]⁺; cyclic voltammetry; electrochemistry; electrocrystallization.

1. Introduction

CuTCNQ exists in two phases with different crystal packing and a significant difference in conductivity.[1] While phase I is a good semiconductor at room temperature with a resistivity of 0.2 S cm⁻¹, phase II is a poor one with a resistivity of 1.3 × 10⁻⁵ S cm⁻¹ (Heintz, 1999).[2] Significantly, CuTCNQ exhibits a reversible switching behavior between the conducting and insulating states upon application of optical irradiation or an electrical field.

The formation of CuTCNQ has been prepared voltammetrically by reducing TCNQ in the presence of Cu⁺ in acetonitrile media or Cu²⁺ in aqueous solution

complex charge transfer process including a TCNQ^{0/-} and Cu^{2+/-} reduction processes as shown in equation 1



The conversion from phase I to phase II material has been observed upon an extensive potential cycling.

However, only CuTCNQ phase I can be detected electrochemically in acetonitrile which gives rise to two redox processes at variable potential and voltammetric time scale relating to the formation of different sizes of crystal as well as morphologies. The formation of CuTCNQF₄ has also been reported (Tran, 2017) .[3] No crystal structure is available for CuTCNQF₄, however this material can be electrocrystallized and characterized on an electrode surface. An exciting finding with the Cu-TCNQF₄ material was that the formation of the more reduced TCNQF₄²⁻ - based material can be detected on voltammetric time scale. The stable dianionic form has not been generated electrochemically for TCNQ. It needs to be stabilized in a coordination polymer with other ligands. For example, numbers of TCNQ²⁻ and TCNQF₄²⁻ coordination polymer were successfully synthesized chemically with the

^aThe University of Danang - University of Science and Education

^bTu Nghia 1 High School, Quang Ngai province

* Corresponding author

Vo Thang Nguyen

Email: vtnguyen@ued.udn.vn

(Neufeld, 2003).[2] The mechanism of the formation of CuTCNQ differs in these two media. In an aqueous solution a solid-solid transformation mechanism with a

diruthenium ligands $\text{Ru}_2(\text{m-CH}_3\text{PhCO}_2)_4$ and $\text{Ru}(\text{o-CF}_3\text{PhCO}_2)_4$ (Kosaka, 2015).[4] Also, the dianionic complexes of TCNQ and TCNQF_4 have been reported with Cu^+ in the presence of other coordination ligands such as 2,6-lutidine, quinone, 2-picoline, 2,2'-bipyridine with H_2TCNQ or H_2TCNQF_4 starting materials (Abrahams, 2015).[5] Electrochemically, the addition of fluorine substituents on TCNQ shifts the reversible potential to more positive values making the TCNQF_4^{2-} more accessible and enhancing its stability.

As part of systematic studies on the electrochemical behavior of fluoro derivatives of TCNQ, the electrochemistry of mono-fluoro TCNQF in the presence of $[\text{Cu}(\text{MeCN})_4]^+$ is now reported. In this study, the reduction of TCNQF to TCNQF^- in the presence of $[\text{Cu}(\text{MeCN})_4]^+$ is described over a range of concentrations and the catalytic activity of a CuTCNQF film on copper foil is compared with that of the other fluoro-TCNQ derivatives.

2. Materials and Methods

2.1. Chemicals

TCNQF (98%, TCI Tokyo), $[\text{Cu}(\text{CH}_3\text{CN})_4]\text{PF}_6$ (98%, Aldrich), acetonitrile (HPLC grade, Omnisolv), isopropanol (BHD) and acetone (suprasolv, Merck KGaA) were used as received from the manufacturer. Bu_4NPF_6 (Aldrich), used as the supporting electrolyte in electrochemical studies, was recrystallized twice from 96% ethanol (Merck) and then dried at 100°C under vacuum for 24 hours prior to use.

2.2. Electrochemistry

Voltammetric experiments were undertaken at room temperature ($22 \pm 2^\circ\text{C}$) using a Bioanalytical Systems (BAS) 100W electrochemical workstation. A standard three electrode cell configuration, comprising a glassy carbon (GC, 1 mm diameter) working electrode, a Ag/Ag^+ reference electrode (RE) and a 1.0 mm diameter platinum wire counter electrode, was employed in those experiments. The working electrode was polished with $0.3 \mu\text{m}$ Al_2O_3 slurry using polishing cloth, washed with water followed by sonication in an ultra sonic bath for 30 seconds prior each run to ensure a fresh electrode surface. The RE consisted of an Ag wire in contact with an acetonitrile solution containing 0.1 M Bu_4NPF_6 and 1.0 mM AgNO_3 , which was

separated from the test solution by a salt bridge. The relative potential of this reference electrode was -124 mV vs the ferrocene/ferrocenium, $\text{Fc}^{+/0}$ couple. All the solutions were purged with nitrogen gas for at least 10 min and a stream of nitrogen was maintained above the solutions during the course of the voltammetric experiments. For bulk electrolysis experiment, a Pt mesh electrode was used as the working electrode instead of a GC electrode.

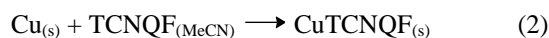
2.3. Synthesis of CuTCNQF

CuTCNQF was prepared electrochemically. A 5.0 ml solution of 0.5 mM TCNQF^- was quantitatively prepared by bulk reduction electrolysis of 5.0 mM TCNQF in acetonitrile (0.1 M Bu_4NPF_6). The potential at Pt mesh working electrode was held at -150 mV vs Ag/Ag^+ until the current ratio reached 1% of the initial value. To this solution, 0.375 ml solution of 100 mM $[\text{Cu}(\text{CH}_3\text{CN})_4]^+$ was added. A dark blue precipitate formed immediately. The mixture was kept stirring was maintained for 10 minutes after which the solid was collected by filtration, washed several times with CH_3CN , dried and stored under vacuum overnight before further characterization.

All the samples generated via these different synthetic pathways were characterized and compared.

2.4. Catalytic experiment

A piece of copper foil was used to prepare a film of CuTCNQF for catalytic experiment according to equation 2.



The foil was initially cleaned by immersion in HNO_3 (5%) to remove surface oxide, then washed with acetone and methanol and dried under a nitrogen stream. To form a layer of CuTCNQF, the copper foil was immersed in a 1.0 mM TCNQF solution in CH_3CN for 12 hours. Afterwards, the foil was removed from the solution, rinsed briefly with CH_3CN to remove excess TCNQF and washed with copious amounts of water. The sample was then dried and stored under vacuum prior to use.

Catalytic activity of CuTCNQF in contact with copper foil (area of 0.16 cm^2) was assessed on the reaction between $\text{S}_2\text{O}_3^{2-}$ and $[\text{Fe}(\text{CN})_6]^{3-}$. A 30 ml solution of 0.1 M $\text{S}_2\text{O}_3^{2-}$ and 1.0 mM $[\text{Fe}(\text{CN})_6]^{3-}$ was stirred in the presence of the CuTCNQF_n film. At

regular time intervals 600 μl of solution was removed for UV-Vis measurement and the amount of $[\text{Fe}(\text{CN})_6]^{3-}$ remaining in the solution was determined by referring to a calibration curve.

2.5. Other instrumentation

UV-Vis spectra were recorded with a Varian Cary 5000 UV-Vis NIR spectrophotometer with a 1.0 cm path length quartz cuvette. A Varian UMA600 IR microscope and FTS7000 optics bench using 128 scans and a resolution of 8 cm^{-1} was used for IR spectra. Raman spectra were recorded on a Renishaw Invia Raman spectrograph with an Argon ion laser excitation at 633 nm.

3. Results and discussion

3.1. The electrochemical synthesis of CuTCNQF in acetonitrile

In order to synthesize CuTCNQF electrochemically, the voltammetry of TCNQF in the presence of $[\text{Cu}(\text{CH}_3\text{CN})_4]^+$ was investigated. The potentials of two reduction processes for TCNQF are well removed from the potentials for the reduction and oxidation of $[\text{Cu}(\text{CH}_3\text{CN})_4]^+$. Hence, the reduction of both reduction steps $\text{TCNQF}^{0/-}$ and $\text{TCNQF}^{-/2-}$ can be studied without any interference from $[\text{Cu}(\text{CH}_3\text{CN})_4]^+$.

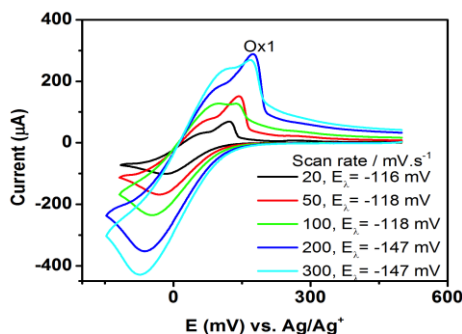


Figure 1. Cyclic voltammograms obtained in acetonitrile ($0.1\text{ M Bu}_4\text{NPF}_6$) for 8.0 mM TCNQF and $8.0\text{ mM }[\text{Cu}(\text{CH}_3\text{CN})_4]^+$ with a 1 mm diameter GC electrode at designated scan rates

The $\text{TCNQF}^{0/-}$ reduction process was studied in an acetonitrile solution containing 8.0 mM TCNQF and $8.0\text{ mM }[\text{Cu}(\text{CH}_3\text{CN})_4]^+$. Voltammograms obtained when the potential was swept negatively to reduce TCNQF to TCNQF^- and then reversed at designated scan rates are shown in Figure 1.

Upon increasing the scan rate from $20\text{ mV}\cdot\text{s}^{-1}$ to $300\text{ mV}\cdot\text{s}^{-1}$ the reduction peak potential shift to more negative from -16 to -76 mV . Furthermore, although the peak current, i_p^{red} , is proportional to the square root of scan rate, $v^{1/2}$, a negative intercept on the current axis was derived which implies that the reduction $\text{TCNQF}^{0/-}$ is not totally diffusion-controlled in the presence of $[\text{Cu}(\text{CH}_3\text{CN})_4]^+$. In the positive scan direction, a new oxidation process, which is sharper and more symmetric, appears at more positive potential (Ox1) than the $\text{TCNQF}^{-/0}$ oxidation step. The Ox1 peak potential (E_p) and current magnitude highly depend on the scan rate as well as the switching potential. For example, E_p shifts positively from 123 to 176 mV when the scan rate increases from 20 to $300\text{ mV}\cdot\text{s}^{-1}$. The loss of diffusion-controlled characteristics together with the appearance of the Ox1 step indicates a chemical step accompanied the reduction of TCNQF to TCNQF^- . It is most likely that solid CuTCNQF is formed via equations (3) and (4).



On this basis, Ox1 peak represents the oxidation of $\text{CuTCNQF}_{(\text{solid})}$ (A) to dissolved TCNQF .

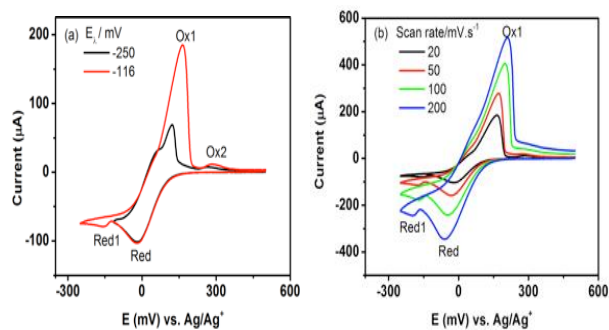


Figure 2. Cyclic voltammograms obtained in acetonitrile ($0.1\text{ M Bu}_4\text{NPF}_6$) for 8.0 mM TCNQF and $8.0\text{ mM }[\text{Cu}(\text{CH}_3\text{CN})_4]^+$ with a 1 mm diameter GC electrode (a) at $20\text{ mV}\cdot\text{s}^{-1}$ as a function of switching potential, (b) switched at -250 mV with designated scan rates

Interestingly, when the potential was scanned to more negative potential before being reversed, at -250 mV , which still avoids the $\text{TCNQF}^{-/2-}$ reduction process found in the absence of Cu^+ , a second reduction process was observed with a small current magnitude (Red1) (see Figure 2).

Simultaneously process Ox1 becomes dominate in the positive potential scan with an enhanced current magnitude of Ox1 which suppresses the diffusion controlled TCNQF⁻⁰ oxidation step. Moreover, a new small broad oxidation peak at 298 mV is now detected. Taken together, these data suggest that more negative potential increases the deposition of the Cu-TCNQF solid associated with the Ox1 step and also enables the formation of another solid which is oxidized at a more positive potential. As illustrated in Figure 2b, at faster scan rates, while the current magnitude of Ox1 increases, the Ox2 peak becomes more difficult to detect which implies that these reductions, leading to solid formation, are kinetically controlled.

The presence of the additional Red1 process is presumably due to the reduction of TCNQF⁰ to TCNQF⁻ at the Cu-TCNQF crystal sites that already formed in Red process followed by the reaction with Cu⁺. The two solids were then oxidized at different potentials.

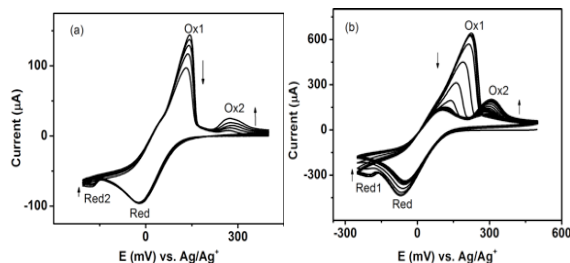


Figure 3. Cyclic voltammograms obtained in acetonitrile (0.1 M Bu₄NPF₆) for 8.0 mM TCNQF and 8.0 mM [Cu(CH₃CN)₄]⁺ with a 1 mm diameter GC electrode when the potential was switched at (a) -205 mV at a scan rate of 20 mV.s⁻¹ (b) switched at -250 mV at a scan rate of 300 mV.s⁻¹

Moreover, on scanning multiple cycles, the nature of the accumulation of solid A (associated with Ox1) and solid B (associated with Ox2) varies (Figure 3). Thus, the Ox2 current magnitude gradually increases on cycling of the potential at scan rates of 20 mV.s⁻¹ and 300 mV.s⁻¹, and Ox1 decreases when the potential was switched at -146 mV (Figure 4) or at -250 mV (Figure 3b). At 300 mV.s⁻¹, the current decay of Ox1 is rapid until it was no longer detected and neither was Red1.

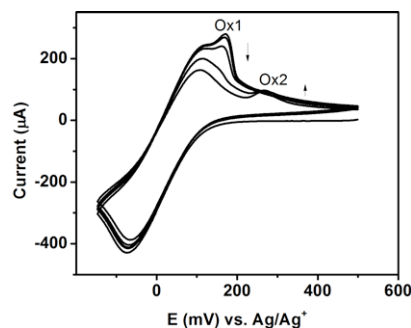


Figure 4. Cyclic voltammograms obtained in acetonitrile (0.1 M Bu₄NPF₆) for 8.0 mM TCNQF and 8.0 mM [Cu(CH₃CN)₄]⁺ with a 1 mm diameter GC electrode when the potential was switched at -146 mV at a scan rate of 300 mV.s⁻¹

These data suggest that the solid product, giving rise to Ox2 oxidation process is thermodynamically more stable than that giving rise to Ox1 process.

From these voltammetric experiments, it is clear that CuTCNQ can be synthesized electrochemically. The bulk materials were generated by adding [Cu(CH₃CN)₄]⁺ into the TCNQF⁻ solution which is formed via bulk electrolysis at -250 mV. Only thermodynamically stable material was obtained.

3.2. Characterization of solids

3.2.1. Spectroscopic characterization

Figure 5 shows IR and Raman spectra of the samples synthesized both electrochemically and chemically on Cu foil. Characteristic IR vibrational bands were detected at 2205 and 2138 cm⁻¹ for the C≡N stretch, 1612 cm⁻¹ for ring C=C stretch, 1504 cm⁻¹ for exocyclic C=C vibration, 1350 cm⁻¹ for the mixing mode of ring C-C and C-F stretch. The C-CN stretch vibrational band was detected at 1196 cm⁻¹. Also, bands at 3343 and 1608 cm⁻¹ imply the existence of water in these materials. Also, Raman absorptions were observed at 2214 cm⁻¹ for the C=N stretch, 1609 cm⁻¹ for the ring C=C stretch and 1391 cm⁻¹ for the exocyclic C=C stretch.

3.2.2. Elemental analysis of CuTCNQF material

Elemental analysis results were found to be C 49.66, H 1.20 and N 19.56% which can be rationalized by the existence of water with an overall composition of CuTCNQF.1/4H₂O (cal. C 49.66, H 1.22 and N 19.30%).

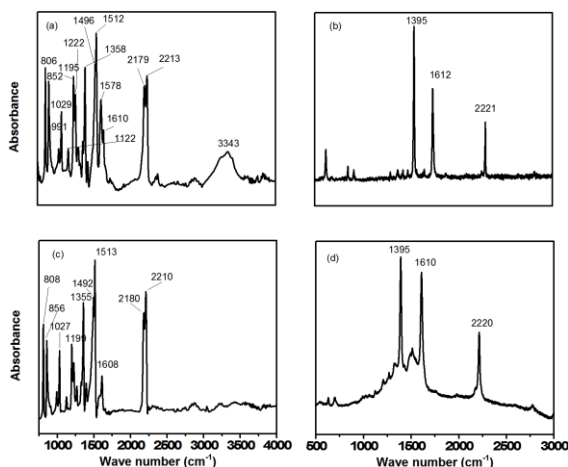
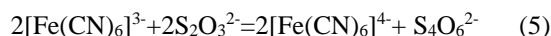


Figure 5. (a) IR and (b) Raman spectra of chemically synthesized CuTCNQF, (c) IR and (d) Raman spectra of electrochemically synthesized CuTCNQF

3.3. Catalytic activity

The redox reaction between ferricyanide and thiosulfate as shown below



was chosen to illustrate the catalytic activity that can be achieved when a CuTCNQF layer on a copper foil presents in the solution.

The rate of the reaction can be monitored by UV-Vis spectrometry using the ferric absorption band at $\lambda_{\text{max}} = 420 \text{ nm}$ using a calibration curve.

This reaction has been shown to be catalysed by colloidal noble metals.[6] Recently, O'Mullane *et al.* also reported the catalytic capability of MTCNQ and MTCNQF₄ (M = Cu, Ag) (Mahajan, 2013).[7]

In order to compare the catalytic activity of CuTCNQF_n derivatives and explore the substituent effect on these catalysts, analogous catalytic experiments were performed by using a film of CuTCNQF on a piece of Cu foil with an area of 0.16 cm². These foils were then added to the mixture of reactants shown in equation 2 while stirring. Aqueous solution of [Fe(CN)₆]³⁻ and S₂O₃²⁻ is yellow and in the absence of the catalyst, the colour does not change over a period of 2 hours. However, the introduction of CuTCNQF leads to rapid loss of the initial yellow colour. This change was quantitatively determined by UV-Vis spectra. The absorbance at 420 was monitored at regular time intervals.

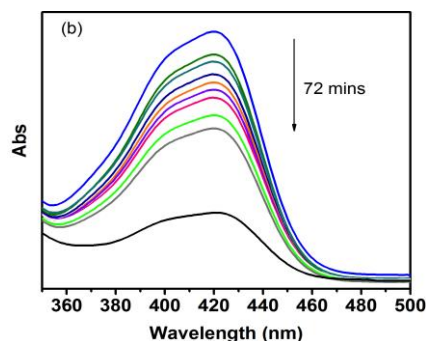


Figure 6. Time dependent UV-Vis spectra of a solution containing 1.0 mM [Fe(CN)₆]³⁻ and 0.1 M S₂O₃²⁻ catalysed by CuTCNQF

As shown in Figure 8, the use of CuTCNQF drives the reaction to a completion state after more than 72 mins (Figure 6).

The catalytic activity depends on several factors, including surface area, material's conductivity or solid-solution interface chemistry. In general, the catalytic reaction is enhanced with catalysts having larger surface area such as nano-materials. CuTCNQ crystal modified with gold nano particles significantly enhances the catalytic activity (Pearson, 2013).[8] The nature of this behaviour needs more investigations to be fully understood.

The composition of the CuTCNQF_n film was compared using IR spectra before and after the catalytic experiment and was found to be identical (Figure 7). This confirm that the surface of the catalyst does not change in its composition after the catalytic reaction.

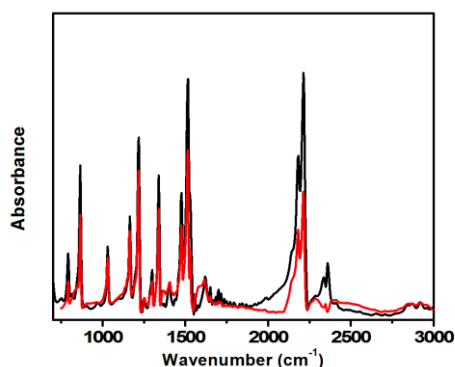


Figure 7. Comparison of the IR spectra of CuTCNQF on a Cu foil before (black) and after (red) catalytic experiment.

4. Conclusion

Cyclic voltammetry of TCNQF in the presence of $[\text{Cu}(\text{MeCN})_4]^+$ in acetonitrile was investigated for reduction processes $\text{TCNQF}^{0/-}$ without any interference from the second process by varying the concentration of TCNQF and $[\text{Cu}(\text{MeCN})_4]^+$. The formation of CuTCNQF was detected in a voltammetric time scale at a concentration of 8.0 mM of TCNQF and $[\text{Cu}(\text{MeCN})_4]^+$. CuTCNQF, unlike other fluoro derivatives, does not possess good catalytic activity on $\text{Fe}^{3+}/\text{S}_2\text{O}_8^{2-}$ redox reaction. This reaction rate with the present of CuTCNQF is as slow as in the presence of CuTCNQ phase II, which is unexpected.

References

- [1] Abrahams B.F., Elliott R.W., Hudson T.A., Robson R., Sutton A.L. (2015). New $\text{CuI}_2(\text{TCNQ-II})$ and $\text{CuI}_2(\text{F}_4\text{TCNQ-II})$ Coordination Polymers. *Crystal Growth & Design*, 15, 5, 2437-2444.
- [2] Heintz R.A., Zhao H., Ouyang X., Grandinetti G., Cowen J., Dunbar K.R. (1999). New Insight into the Nature of $\text{Cu}(\text{TCNQ})$: "Solution Routes to Two Distinct Polymorphs and Their Relationship to Crystalline Films That Display Bistable Switching Behavior". *Inorganic Chemistry*, 38, 1, 144-156.
- [3] Kosaka W., Morita T., Yokoyama T., Zhang J., Miyasaka H. (2015). Fully Electron-Transferred Donor/Acceptor Layered Frameworks with TCNQ^{2-} , *Inorganic Chemistry*, 54, 4, 1518-1527.
- [4] Mahajan M., Bhargava S.K., O'Mullane A.P. (2013). Reusable surface confined semi-conducting metal-TCNQ and metal-TCNQF4 catalysts for electron transfer reactions. *RSC Advances*, 3, 13, 2013, 4440-4446.
- [5] Tran Duc Manh, Vo Thang Nguyen, Le Tu Hai (2017). Nghiên cứu tổng hợp hợp chất mới CuTCNQF_4^{2-} . *Tạp Chí Khoa học Công nghệ ĐHQĐN*, 3, 112, 34-39.
- [6] Neufeld A.K., Madsen I., Bond A.M., Hogan C.F. (2003). Phase, Morphology, and Particle Size Changes Associated with the Solid-Solid Electrochemical Interconversion of TCNQ and Semiconducting CuTCNQ ($\text{TCNQ} = \text{Tetracyanoquinodimethane}$). *Chemistry of Materials*, 15, 19, 3573-3585.
- [7] Pearson A., Bansal V., O'Mullane A.P. (2013). Lateral charge propagation effects during the galvanic replacement of electrodeposited MTCNQ ($M = \text{Cu}, \text{Ag}$) microstructures with gold and its influence on catalyzed electron transfer reactions. *Electrochimica Acta*, 114, 189-197.

NGHIÊN CỨU TỔNG HỢP ĐIỆN HOÁ HỢP CHẤT CuTCNQF VÀ ĐÁNH GIÁ HOẠT TÍNH XÚC TÁC CỦA NÓ

Tóm tắt: Các thí nghiệm cực phổ vòng tuần hoàn được sử dụng để nghiên cứu các quá trình oxi hoá khử thứ nhất $\text{TCNQF}^{0/-}$ xảy ra trong dung dịch có chứa TCNQF và $[\text{Cu}(\text{MeCN})_4]^+$. Các thí nghiệm đã cho thấy quá trình khử này có thể được theo dõi mà không chịu ảnh hưởng của quá trình khử thứ hai. Trong quá trình quét thế, sự hình thành của chất rắn CuTCNQF đã được ghi nhận khi nồng độ của TCNQF và $[\text{Cu}(\text{MeCN})_4]^+$ là 8,0 mM. Đặc biệt, trong quá trình thực nghiệm đã nhận thấy sự hình thành của hai pha khác nhau của CuTCNQF với bằng chứng là sự xuất hiện của một sóng cực phổ không thuận nghịch. Hợp chất mới này đã được tổng hợp bằng phương pháp hoá học và điện hoá và được khảo sát tính chất bằng phương pháp phổ IR và Raman. Không giống các dẫn xuất flo khác, khả năng xúc tác của CuTCNQF đối với hệ oxi hoá khử $\text{Fe}^{3+}/\text{S}_2\text{O}_8^{2-}$ không cao. Vận tốc phản ứng này khi có mặt CuTCNQF chỉ tương đương với CuTCNQ pha II.

Từ khóa: TCNQF; $[\text{Cu}(\text{MeCN})_4]^+$; cực phổ vòng tuần hoàn; điện hoá học; kết tinh điện hoá.